

RESEARCH ARTICLE

Experimental Validation of Artificial Neural Network Based Road Condition Classifier and Its Complementation

DAEYI JUNG 

Department of Mechanical and Automotive Engineering, Kunsan National University, Gunsan-si 54150, South Korea

e-mail: djjung@kunsan.ac.kr


This work was supported in part by the Korea Institute for Advancement of Technology (KIAT) funded by the Korean Government (MOTIE) through the Development of Integrated Electro-Mechanical Braking System Based on Redundancy Design under Grant 20015450, and in part by KIAT funded by the Korean Government (MOTIE) through the Development of Integrated Longitudinal and Lateral Safety Control System Based on Forward Collision Prediction for Midsize and Small Commercial Vehicles Responding Safety Regulations under Grant P0018565.

ABSTRACT Our previous study focused on the development of artificial neural network (ANN) classifier estimating the maximum static road friction coefficient for each wheel of the vehicle based on the Carsim/Simulink co-simulation environment by utilizing only existing sensor value without additional sensors. As follow-up to the previous study, this paper investigates the effectiveness of the proposed ANN classifier using the field test data in Software-In-Loop-Simulation (SILS) environment. Furthermore, we have extended the input of ANN classifier to improve an estimation performance. Specifically, the braking pressure and pressure gradient of each wheel were additionally set as the new inputs of the classifier (cf. the original inputs are the initial speed at braking, the vehicle deceleration, the wheel slip ratio, and the vehicle mass). Hence, the benefits of additional inputs have been clearly explored here. Moreover, the proposed scheme was challenged to other, more complicate road surface conditions (including jump and split friction roads). The original classifier guarantees a fairly accurate estimate, but we found that including brake pressure information into the classifier yielded estimates in better quality and the estimation results capture 86~95% accuracy for normal braking regardless of roads and 70~84% accuracy for extreme road conditions. This work will be a valuable asset for those who wish to develop the practical estimation methods for road friction coefficient via an ANN classifier using only inertial sensor information already available in most standard cars.

INDEX TERMS Braking, road friction coefficient, estimations, data training, artificial neural network (ANN) classifier.

I. INTRODUCTION

Most active safety systems benefit from a reliable and robust estimation of road surface condition (or friction coefficient μ). Especially, the road/tire surface information is essential for a braking of vehicle and a tracking precision of potential trajectories, leading to a better vehicle control management. However, since the interaction between the tire and the road surface is indirect and highly non-linear, it is

The associate editor coordinating the review of this manuscript and approving it for publication was Jjun Cheng .

difficult to accurately and immediately estimate the road surface condition. Consequently, many various studies of tire-road friction modeling and estimation have been conducted.

First, many studies proposed friction coefficient identification strategies based on the concept “slip-slope” [1], [2], [3], [4]. In all the approaches discussed above, the research results only focused on the estimation of the average tire-road friction coefficient for the entire vehicle. Furthermore, [5] utilizes a differential GPS and a nonlinear longitudinal tire force model to estimate road friction coefficient and [6] develops a rules-based μ -estimation algorithm where aims

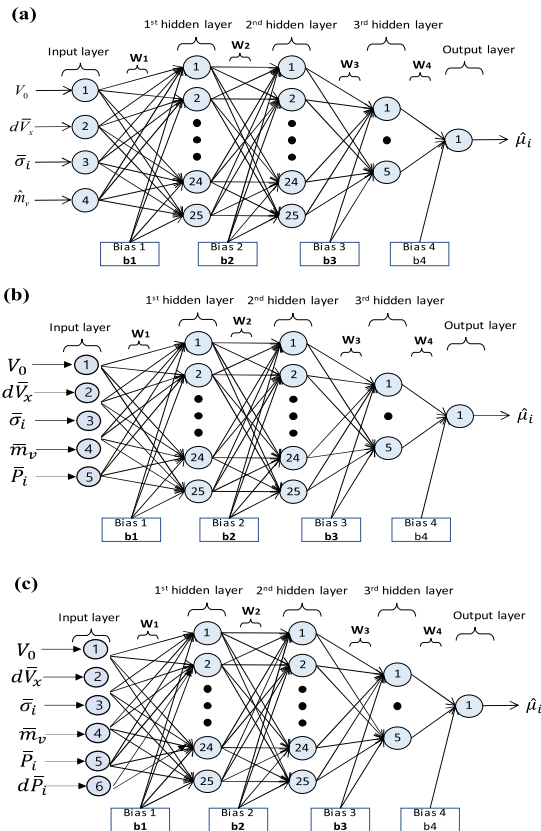


FIGURE 1. Proposed ANN structure for each wheel (a) 4-input ANN classifier, (b) 5-input ANN classifier, and (c) 6-input ANN classifier.

at estimating the tire/road friction coefficient during braking avoiding a particular tire-model. Reference [7] presented the estimation approach based on the relationship between the wheel slip ratio and the friction coefficient using both an effective tire radius observer and a tire normal force observer. Reference [8] proposed a novel μ slip curve using a nonlinear curve fitting technique. Furthermore, [9], [10], [11] present the adaptive friction coefficient estimation methods combining the longitudinal/lateral/coupled vehicle dynamics-responses according to different road surfaces. Reference [9] identified the road friction coefficient using longitudinal vehicle model and LuGre/Burckhardt tyre-road friction models along with RLS. Reference [10] estimates tire-road friction coefficient of a vehicle on the basis of lateral dynamics of the vehicle with Kalman filter (KF). [11] presents the estimation approach via UKF based on interactive longitudinal and lateral vehicle models. Also, [12] provides the holistic reviews of the tire-road models and methods used for tire/road friction coefficient estimation. However, these methods [5], [6], [7], [8], [9], [10], [11] usually rely on reduced-order mathematical models between the vehicle/tires and the road surface, which are insufficient to fully describe the exact relationship, often resulting in the outcomes with unacceptable accuracy. Other approaches using vision/optical sensors or acoustic devices for μ estimation [13], [14], [15]

TABLE 1. Max. number of outliers for each road (training results).

| Road classification | Max. Outliers |
|----------------------------------|------------------|
| Icy road ($\mu < 0.2$) | 2 of 180 (1%) |
| Snowy road ($0.2 < \mu < 0.5$) | 5 of 200 (2.5%) |
| Asphalt road ($\mu > 0.8$) | 5 of 170 (2.95%) |

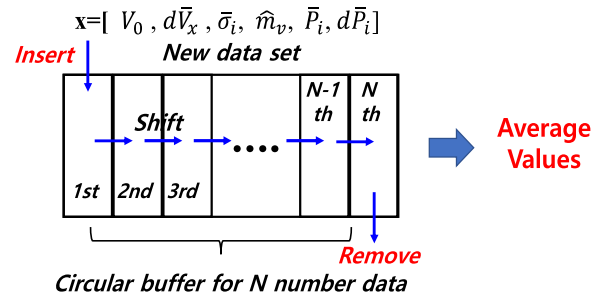


FIGURE 2. Circular buffer for continuous averaging of N-number data every sampling time.

are also explored. Reference [13] proposed a new predictive methodology for the μ -estimation by using a camera and a microphone. References [14] and [15] measured the wetness of the road by detecting reflected light using optical sensors. However, these methods depend on the intensity of light or sound (sensitive to surroundings) and the additional sensors are required to serve this purpose.

Recently, to compensate for the shortcomings of the tire model and vehicle dynamics-based method, machine-learning and deep learning techniques along with vision system were employed [16], [17], [18], [19], [20], [21], [22], [23], [24]. Reference [16] employed Neural Network to identify the tire and wheel suspension behavior and similarly [17] proposed a solution for an optimization problem in which a tire model describing the interaction between tire and road surface using genetic algorithm. Reference [18] provided a mapping from input parameters to the maximum road friction coefficient with general regression neural network, effectively avoiding complicated tire models. Reference [19] used the time-delay neural network to estimate a road friction, which becomes more robust. Moreover, the gated recurrent unit (GRU) network has been used to fulfill the purpose [20]. [21] presents a road identification method using video images and DNN (Deep Learning Network) techniques for the purpose of collaboration with ABS. Reference [22] describes Neural Network approach for slip-slope prediction using a low-cost camera, vehicle GPS and other basic vehicle sensors. Reference [23] compared several machine learning methods (a convolutional neural network, a shallow neural network, a long short-term memory network and an ensemble of bagged decision trees) for road friction estimation and verified that the convolutional neural network and shallow neural network had the best performance. In associated with [16], [17], [18], [19], [20], [21], [22], and [23] but partially unlike those, our previous work [24] focused on machine learning

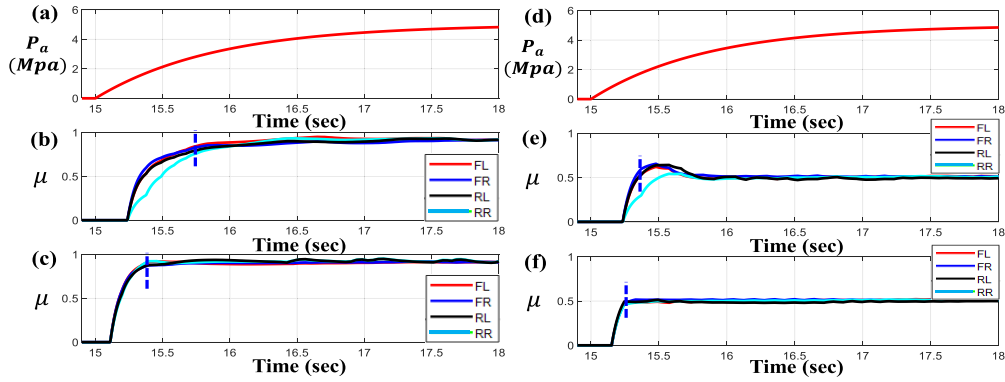


FIGURE 3. Simulation results of 4-input ANN classifier and 6-input ANN classifier for each wheel (a) Brake Scenario for $\mu = 0.9$, (b) Result of 4-input for $\mu = 0.9$, (c) Result of 6-input for $\mu = 0.9$, (d) Brake Scenario for $\mu = 0.5$, (e) Result of 4-input for $\mu = 0.5$ and (f) Result of 6-input for $\mu = 0.5$.

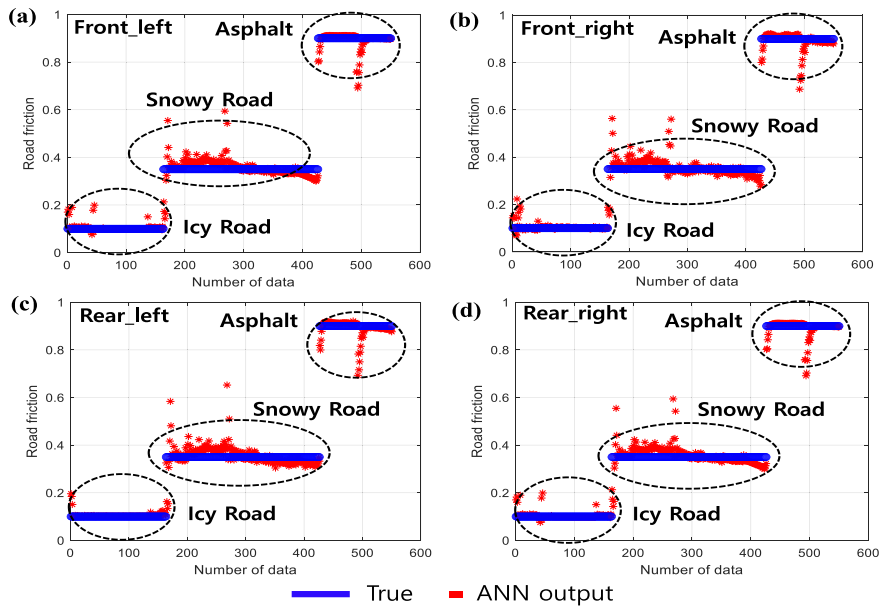


FIGURE 4. Training results of 6-input ANN classifier for each wheel (a) Result of Front-Left Wheel, (b) Result of Front-Right Wheel, (c) Result of Rear-Left Wheel and (d) Result of Rear-Right Wheel.

based ANN classifier for road friction coefficient estimation using only the inertial information of existing sensors (w/o any additional sensors), and the effectiveness of classifier has been addressed via the simulation results. Therefore, this paper validates our previous work using actual field-test data in SILS environment and includes the complementation to obtain the estimation results in better quality. The contributions of this study are followed by, i) There is a lack of machine learning research using only inertial sensor information for road friction estimation under the current trend that most of studies focus on deep-learning with vision system, thus we try to maximize the estimation performance based on the ANN classifier with the existing sensor values. ii) The effectiveness of previous ANN-based classifier [24] has been validated using real test data and we found some features to be further improved although it guarantees a certain level of

performance. iii) In order to compensate such deficiencies, the information on brake pressure has been set as another input of ANN classifier. The effectiveness of this modification has been also challenged by the field test data. iv) It is found that the proposed estimation scheme guarantees quicker estimation response and smoother results compared to the previous approach (i.e, without using brake pressure as the input). v) To reduce the computational load of the ANN classifier and to implement it in the cost-effective commercial ECU in a future, we employed the circular buffer for data pre-processing, and explored a reasonable minimum number of neurons in the classifier while ensuring overall estimation accuracy. The rest of this paper is organized as follows: **Section II** briefly introduced the ANN-based road classifier proposed in [24] and explained its modification to obtain better results. **Section III** presents the validation of proposed

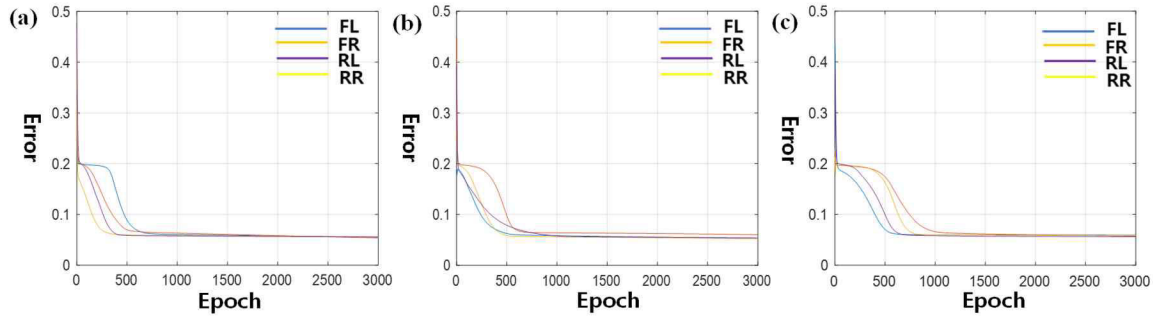


FIGURE 5. Training errors of 6-input ANN classifier based on different total number of neurons (a) Result of 200 neurons, (b) Results of 100 neurons, and (c) Result of 40 neurons.

TABLE 2. Actual test vehicle configuration.

| Vehicle model | Specification |
|-----------------------------|-----------------|
| Type | E-class |
| Brake | ABS at 4 wheels |
| Powertrain | 150kW, 6 speeds |
| Tires | 215/55 R17 |
| Suspension | Independent |
| Total mass of empty vehicle | 2150 kg |



FIGURE 6. Actual vehicle for road-test and validation process (SILS environment).

work with the real test data. Finally, the conclusions have been made.

II. ANN-BASED ROAD FRICTION CLASSIFIER

The methodologies to design and implement ANN-based road friction classifier are specifically presented in our previous study [24]. Therefore, in this section, the structure of ANN classifier is briefly introduced. In addition, in order to further improve the estimation performance through real-vehicle tests, the extension of inputs for the existing classifier was proposed.

In Fig.1, the structures of three classifiers are described with the different inputs. Fig.1(a) represents the original classifier [24] with the 4-input $\mathbf{x} = [V_0 d\bar{V}_x \bar{\sigma}_i \hat{m}_v]^T \in \mathfrak{R}^{4 \times 1}$, where V_0 is the initial velocity at the braking moment, $d\bar{V}_x$ is the average gradient of vehicle’s velocity during the deceleration within a defined data interval (WDDI), $\bar{\sigma}_i$ (for $i = FL, FR, RL, RR$) is the average slip ratio of each wheel WDDI, and \hat{m}_v is the vehicle mass. Fig.1(b) describes the

classifier with the 5-input $\mathbf{x} = [V_0 d\bar{V}_x \bar{\sigma}_i \hat{m}_v \bar{P}_i]^T \in \mathfrak{R}^{5 \times 1}$, where \bar{P}_i is the average braking pressure for each wheel (for $i = FL, FR, RL, RR$) WDDI. And, Fig.1(c) displays the classifier with the 6-input $\mathbf{x} = [V_0 d\bar{V}_x \bar{\sigma}_i \hat{m}_v \bar{P}_i d\bar{P}_i]^T \in \mathfrak{R}^{6 \times 1}$, where $d\bar{P}_i$ is the average gradient of braking pressure for each wheel WDDI. Since the original ANN classifier (Fig.1(a)) does not include a braking pressure as an input, its performance may deteriorate depending on the different braking scenarios generated by various drivers, even though it can be still and effectively used for an ABS or an Automatic Emergency Braking (AES) operated by controlled braking scenarios. In addition, the estimate via this classifier would not be smooth on actual vehicle test, since it is directly affected by irregular wheel slip ratio values $\bar{\sigma}_i$ and does not influenced by the braking pressure information which is immediate and direct braking response. Moreover, it shows less accurate results when the applied brake pressure for each wheel is relatively low. These viewpoints are addressed by the Carsim/Simulink simulation results in Fig.3 and will be further addressed in the next Section using actual test data. Fig.3 includes two cases of simulations. Fig.3 (b)-(c) are the results of 4 and 6-input for the condition $\mu = 0.9$ while Fig.3 (e)-(f) are the outcomes of 4 and 6-input for $\mu = 0.5$. The braking scenario used here is to slowly increase a brake pressure. As shown in Fig.3, the estimates are relatively inaccurate at the low brake pressure (i.e, in the early stage of braking) but the case via 6-input could capture the desired value quicker than the one via 4-input. This means that the case with 4 inputs is less sensitive to capture the proper estimation for the low braking pressure. Therefore, with these points, we extended the ANN structure to accept more inputs for encountering the information about the braking scenario. The proposed ANN classifier in Fig.1(b) adopts the 5-inputs by adding another input, the average braking pressure for each wheel, \bar{P}_i , and the classifier in Fig.1(c) accepts one more input, the average gradient of braking pressure for each wheel, $d\bar{P}_i$. Brake pressure on each wheel is available on most of modern cars since ABS and ESP are mandatory on cars for safety concerns. Those two classifiers in Fig.1(b) and Fig.1(c) generate immediate estimation responses since they utilize most direct braking information, resulting in quick estimation

performance even when various braking scenarios including low levels of braking pressure are applied. In the following section, we also validated these views, and will compare and evaluate the performances of the three classifiers shown in Fig. 1. Before proceeding, how the classifier's input is computed is specified below (i.e, pre-processing of raw data).

$$d\bar{V}_x = \begin{cases} \frac{1}{N} \sum_{t=1}^N (V_{x,t} - V_{x,t-1}) / \Delta t, & 0.2 \text{ km/h} < V_x < 0.99 V_0 \\ d\bar{V}_x, V_x < 0.2 \text{ km/h} \end{cases} \quad (1)$$

where, N is the numbers of data to obtain the average value and selected as 10 for this study. Due to the noise of data, the averaging process is important to avoid unwanted results, and it should be noted that the circular buffer (insert, shift and removal processes) is employed for continuously averaging of N -number of data at every sampling time, as shown in Fig.2. Also, V_0 is the vehicle velocity captured at the first moment of braking and, Δt indicates the size of sampling time.

The average slip ratio of each wheel $\bar{\sigma}_i$ (for $i = \text{FL, FR, RL, RR}$) are also calculated by,

$$\bar{\sigma}_i = \begin{cases} \frac{1}{N} \sum_{t=1}^N (\sigma_{it} - \sigma_{i,t-1}), & 0.2 < V_x < 0.99 V_0 (\text{km/h}) \\ \bar{\sigma}_i, & V_x < 0.2 \text{ km/h for } i = \text{FL, FR, RL, RR} \end{cases} \quad (2)$$

To implement ANN classifier shown in Fig.1 (b) and (c), the average pressure and the average gradient of pressure for each wheel are respectively prepared as the inputs in the following manners.

$$\bar{P}_i = \begin{cases} \frac{1}{N} \sum_{t=1}^N (P_{it} - P_{i,t-1}), & 0.2 < V_x < 0.99 V_0 \\ \bar{P}_i, & V_x < 0.2 \text{ km/h for } i = \text{FL, FR, RL, RR} \end{cases} \quad (3)$$

$$d\bar{P}_i = \begin{cases} \frac{1}{N} \sum_{t=1}^N (P_{i,t} - P_{i,t-1}) / \Delta t, & 0.2 < V_x < 0.99 V_0 \\ d\bar{P}_i, & V_x < 0.2 \text{ km/h for } i = \text{FL, FR, RL, RR} \end{cases} \quad (4)$$

As the final step, in order to use these as the inputs for ANN classifier, the normalization should be conducted by dividing them via the maximums and is followed by $\mathbf{x} = [V_0/V_{max}, d\bar{V}_x/dV_{max}, \bar{\sigma}_i, \hat{m}_v/\hat{m}_{v,max}, \bar{P}_i/\bar{P}_{max}, d\bar{P}_i/d\bar{P}_{max}] \in \mathfrak{R}^{6 \times 1}$, where the above maximums are determined by the car manufacture's specification but can be adjusted for own sake.

Furthermore, the mathematical expression of 4-layer ANN classifier in [24] is briefly reviewed by,

$$\hat{\mu} = f_4(\mathbf{W}_4 f_3(\mathbf{W}_3 f_2(\mathbf{W}_2 f_1(\mathbf{W}_1 \mathbf{x} + \mathbf{b}_1) + \mathbf{b}_2) + \mathbf{b}_3) + \mathbf{b}_4) \in \mathfrak{R} \quad (5)$$

where $\mathbf{x} \in \mathfrak{R}^{n \times 1}$ is the input of the proposed ANN classifier. And, $\mathbf{W}_1 \in \mathfrak{R}^{m \times n}$, $\mathbf{W}_2 \in \mathfrak{R}^{m \times m}$, $\mathbf{W}_3 \in \mathfrak{R}^{m \times m}$, and $\mathbf{W}_4 \in \mathfrak{R}^{m \times 1}$ are the weight matrixes (or vectors) of the first hidden layer, the second hidden layer, the third hidden layer, and the output layer, respectively. $\mathbf{b}_1 \in \mathfrak{R}^{n \times 1}$,

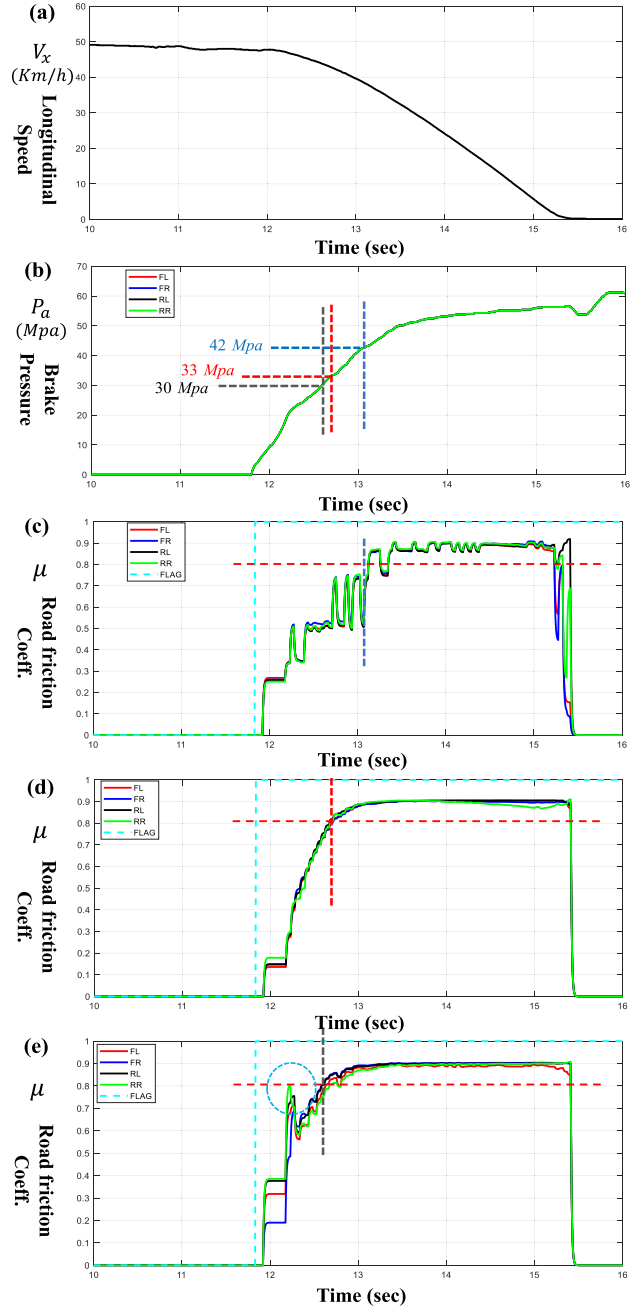


FIGURE 7. Estimation results of asphalt road ($\mu > 0.8$) for braking at $V_0 = 50 \text{ km/h}$ (a) Vehicle longitudinal speed V_x (b) Brake Pressure for all wheels (c) 4-input estimation results ($V_0 d\bar{V}_x \bar{\sigma}_i \hat{m}_v$) (d) 5-input estimation results ($V_0 d\bar{V}_x \bar{\sigma}_i \hat{m}_v \bar{P}_i$), and (e) 6-input estimation results ($V_0 d\bar{V}_x \bar{\sigma}_i \hat{m}_v \bar{P}_i d\bar{P}_i$).

$\mathbf{b}_2 \in \mathfrak{R}^{m \times 1}$, $\mathbf{b}_3 \in \mathfrak{R}^{m \times 1}$, $\mathbf{b}_4 \in \mathfrak{R}$ are the bias vectors (or scalar) of the three hidden layers and the output layer. For more detail of ANN classifier including the tuning algorithm and the selected activation functions, see [24]. Fig.3 represents the training results of 6-input ANN classifier for each wheel according to the three type of roads, an asphalt road, a snowy road, as well as an icy road. Here, it should be noted that each road contains two separate data set. According to

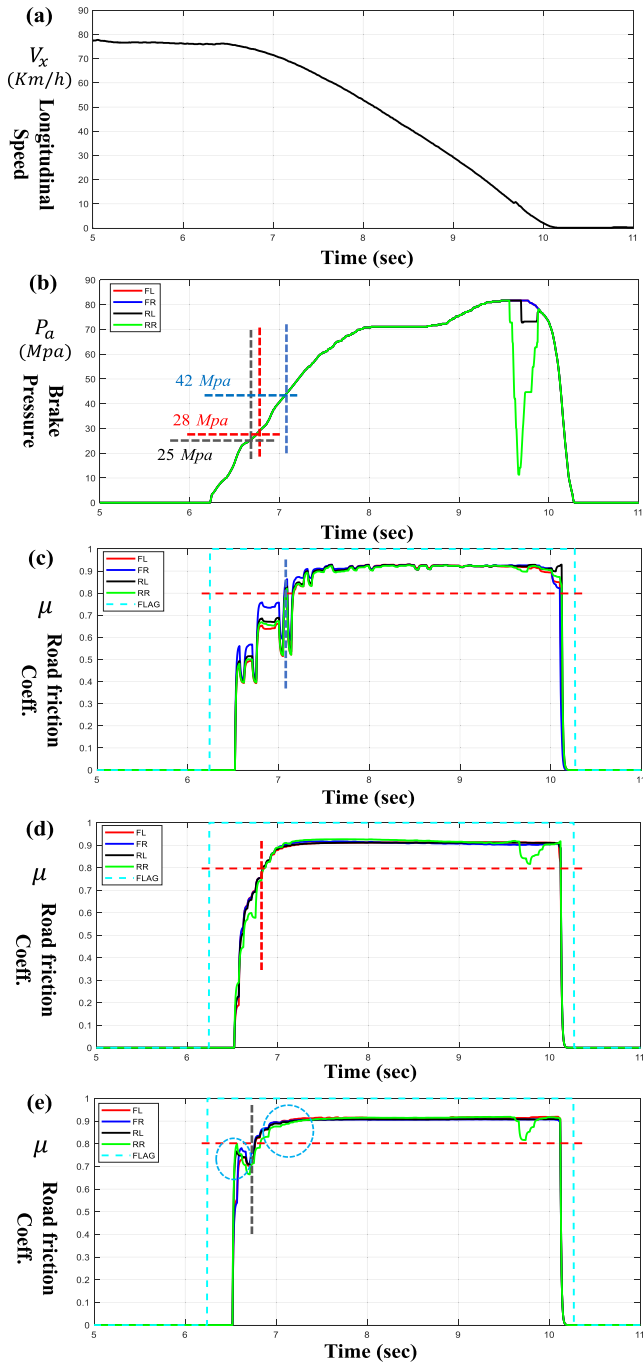


FIGURE 8. Estimation results of asphalt road ($\mu > 0.8$) for braking at $V_0 = 80\text{km/h}$ (a) Vehicle longitudinal speed V_x (b) Brake Pressure for all wheels (c) 4-input estimation results ($V_0 dV_x \bar{\sigma}_i \hat{m}_v$) (d) 5-input estimation results ($V_0 dV_x \bar{\sigma}_i \hat{m}_v \hat{P}_i$), and (e) 6-input estimation results ($V_0 dV_x \bar{\sigma}_i \hat{m}_v \hat{P}_i d\hat{P}_i$).

Fig.3, it is found that the training results are well matched with the true references and the accuracy is almost 97% relative to the references (approximately, 12 outliers out of 550 data points, and see Table.1 for more detail).

The true references are determined by the average friction values of each road. For an asphalt road, the reference value is assumed as 0.9 since it ranges from 0.8 to 1 for

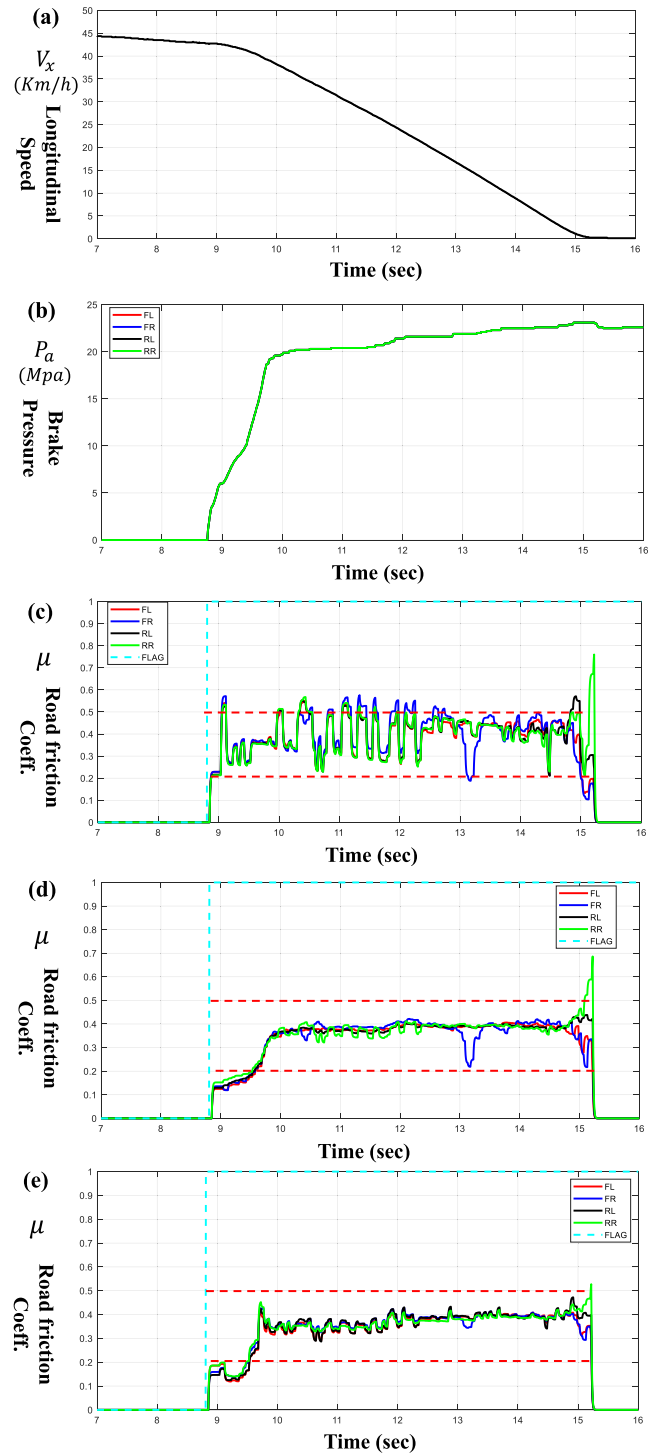


FIGURE 9. Estimation results of snowy road ($0.2 < \mu < 0.5$) for braking at $V_0 = 45\text{km/h}$ (a) Vehicle longitudinal speed V_x (b) Brake Pressure for all wheels ($V_0 dV_x \bar{\sigma}_i \hat{m}_v$) (c) 4-input estimation results ($V_0 dV_x \bar{\sigma}_i \hat{m}_v$) (d) 5-input estimation results ($V_0 dV_x \bar{\sigma}_i \hat{m}_v \hat{P}_i$), and (e) 6-input estimation results ($V_0 dV_x \bar{\sigma}_i \hat{m}_v \hat{P}_i d\hat{P}_i$).

dry asphalt road. A snowy road is assumed to be referenced as 0.35 since it approximately ranges from 0.2 to 0.5. For an icy road, the value is assumed as 0.1 since it ranges below 0.2. Fig.4 explores the training errors of 6-input ANN

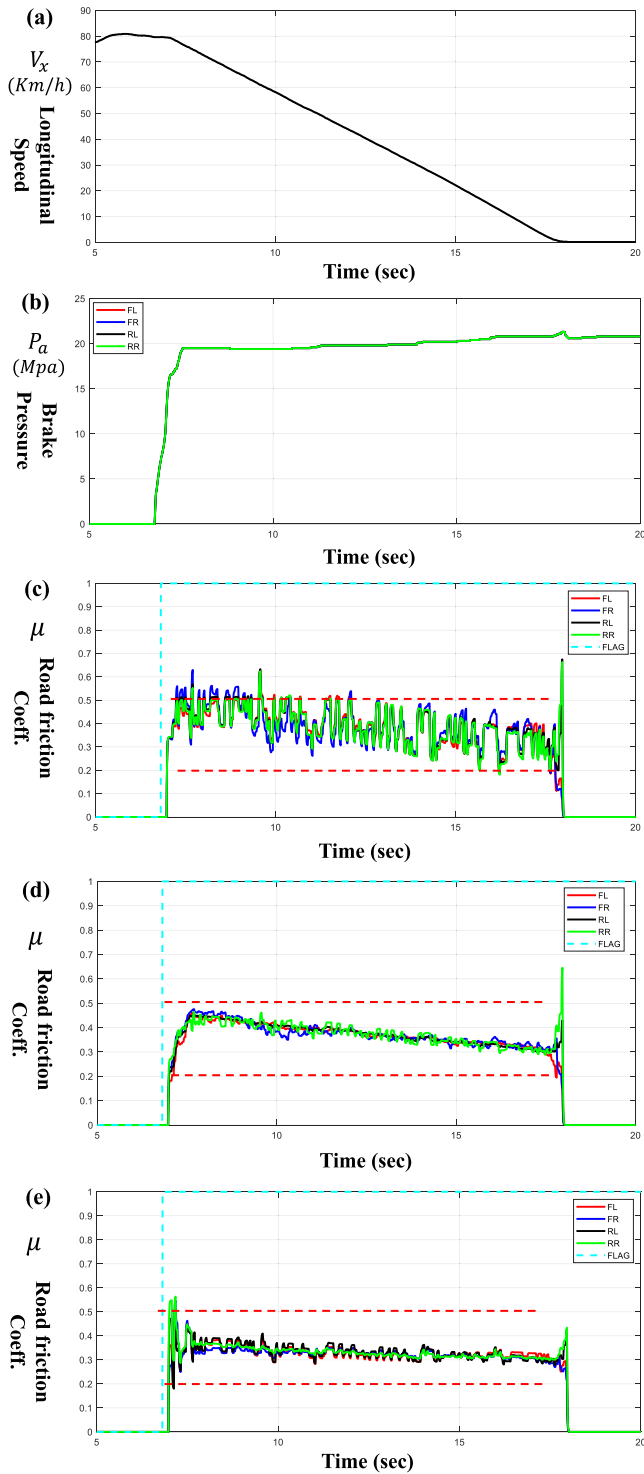


FIGURE 10. Estimation results of snowy road($0.2 < \mu < 0.5$) for braking at $V_0 = 80\text{km/h}$ (a) Vehicle longitudinal speed V_x (b) Brake Pressure for all wheels (c) 4-input estimation results ($V_0 d \bar{V}_x \bar{\sigma}_i \hat{m}_v$) (d) 5-input estimation results ($V_0 d \bar{V}_x \bar{\sigma}_i \hat{m}_v \bar{P}_i$), and (e) 6-input estimation results ($V_0 d \bar{V}_x \bar{\sigma}_i \hat{m}_v \bar{P}_i d \bar{P}_i$).

classifiers according to the total number of neurons in all layers, 200 neurons, 100 neurons and 40 neurons.

Regardless of number of neurons, all training errors converged below 0.07(Although the errors converge quickly for

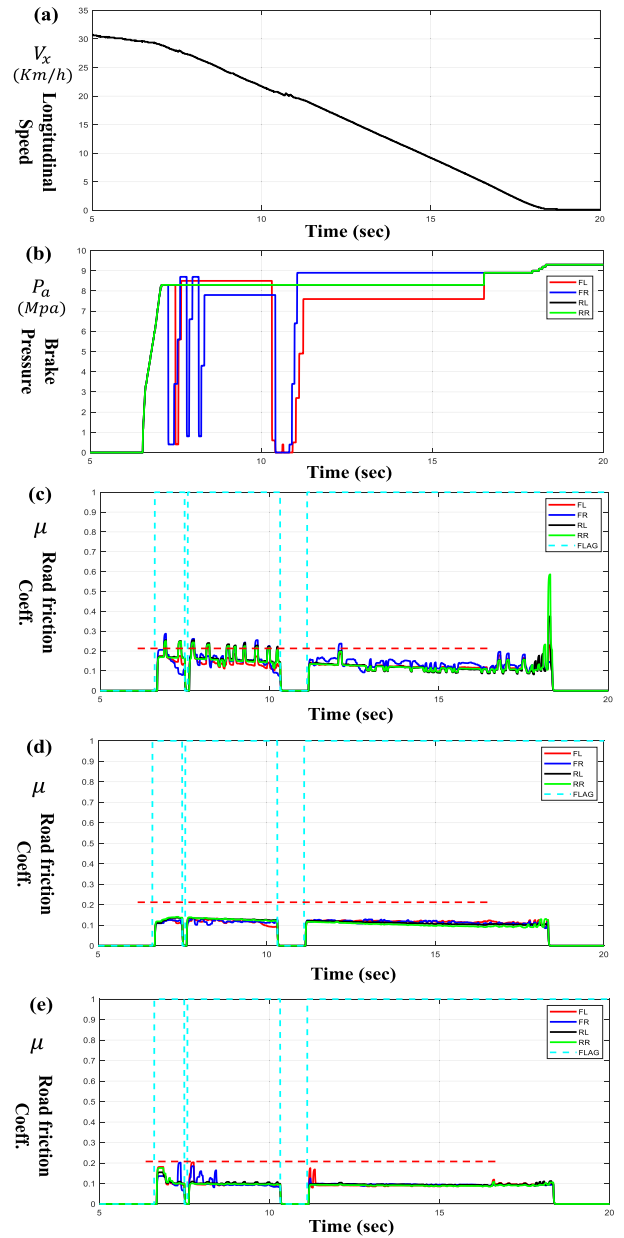


FIGURE 11. Estimation results of icy road($\mu < 0.2$) for braking at $V_0 = 30\text{km/h}$ under partial ABS operation (a) Vehicle longitudinal speed V_x (b) Brake Pressure for all wheels (c) 4-input estimation results ($V_0 d \bar{V}_x \bar{\sigma}_i \hat{m}_v$) (d) 5-input estimation results ($V_0 d \bar{V}_x \bar{\sigma}_i \hat{m}_v \bar{P}_i$), and (e) 6-input estimation results ($V_0 d \bar{V}_x \bar{\sigma}_i \hat{m}_v \bar{P}_i d \bar{P}_i$).

more neurons). It is found that the case with the least number of neurons among those three is also sufficient to capture the nonlinearity between tire and road during braking. Therefore, due to the fact that the computational load will be expensive if more neurons are involved, the last case (40 neurons) was chosen.

III. EXPERIMENTAL VALIDATION

In this section, we investigated the effectiveness of proposed ANN classifier based on various field test performed at three representative road surfaces, asphalt, snowy, and icy roads

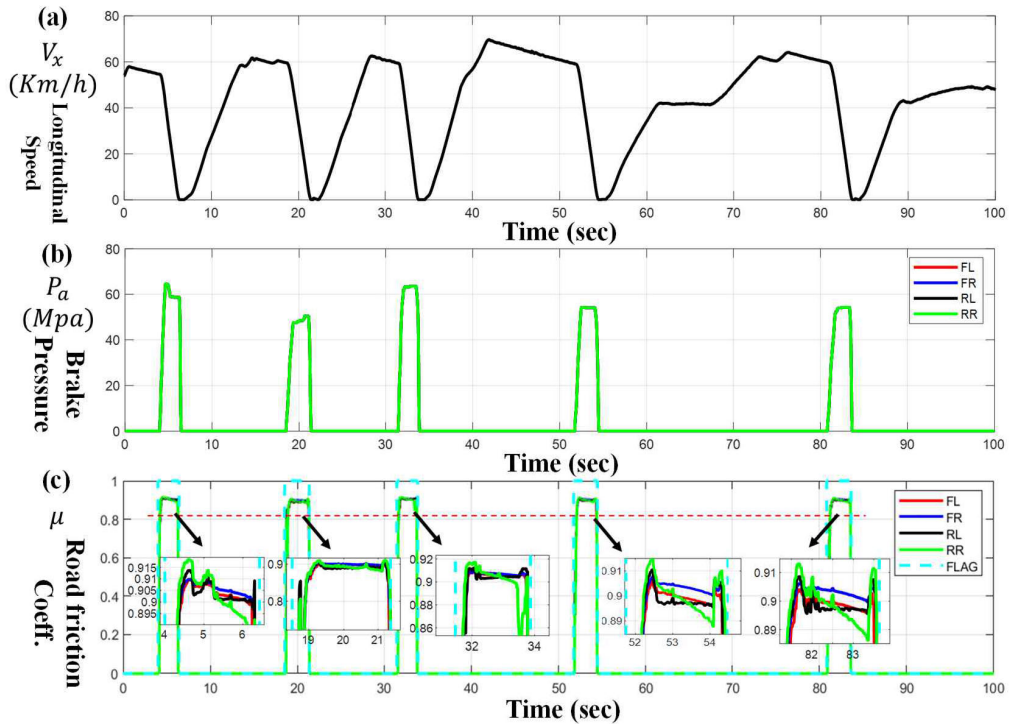


FIGURE 12. Estimation results of asphalt road ($\mu > 0.8$) (a) Vehicle longitudinal speed V_x (b) Brake Pressure for all wheels and (c) 6-input estimation results ($V_0 dV_x \bar{a}_i \hat{m}_v P_i dP_i$).

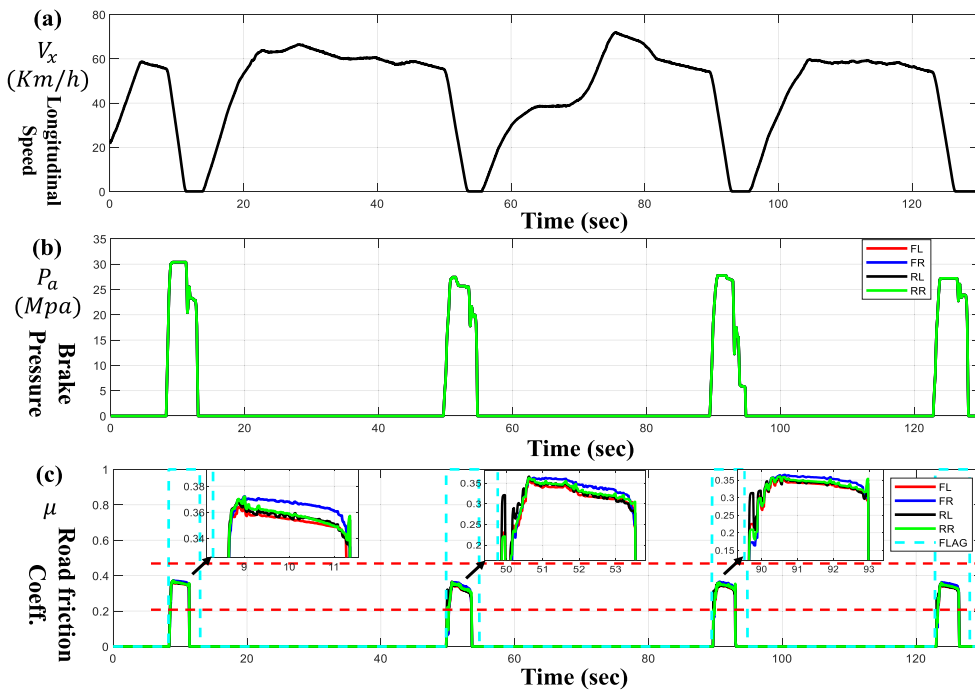


FIGURE 13. Estimation results of snowy road ($0.2 < \mu < 0.5$) (a) Vehicle longitudinal speed V_x (b) Brake Pressure for all wheels and (c) 6-input estimation results ($V_0 dV_x \bar{a}_i \hat{m}_v P_i dP_i$).

along with several different braking scenarios including the case with partial or full ABS operation. The vehicle used for the test and the validation process (Software-In-Loop-Simulation (SILS) based on field test data) are displayed in

Fig.6, and the brief configuration of vehicle is presented in Table.2.

Fig.7 presents the estimation results of asphalt road ($\mu > 0.8$) for braking at approximately $V_0 = 50\text{km/h}$.

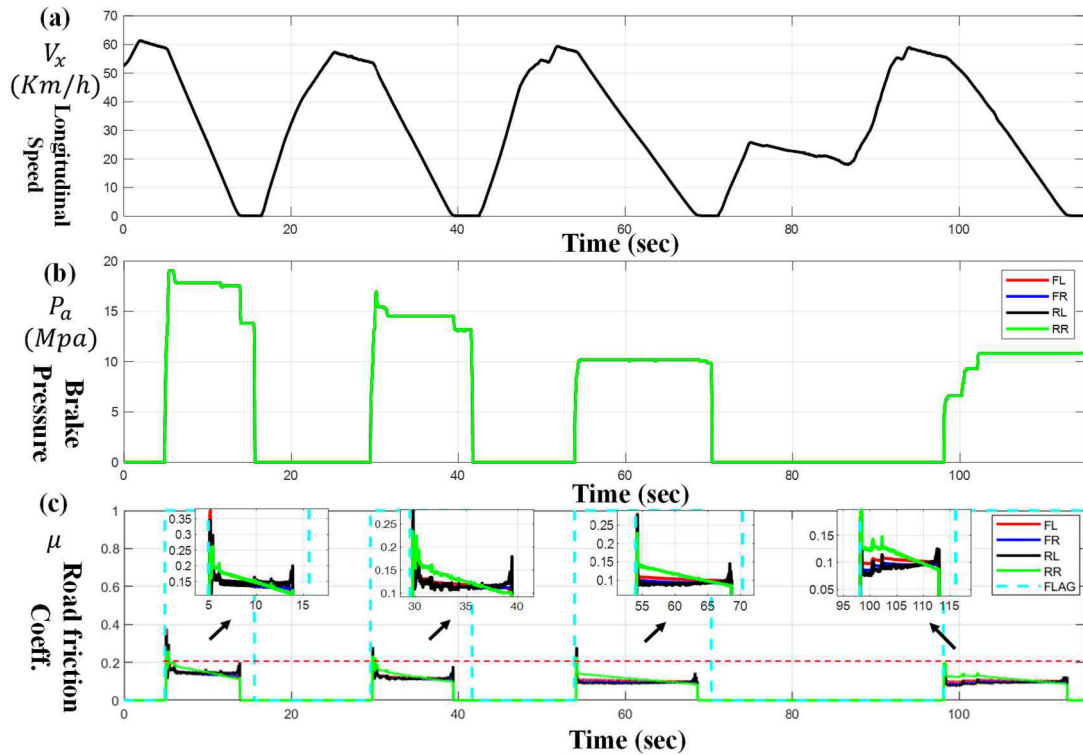


FIGURE 14. Estimation results of icy road($\mu < 0.2$) (a) Vehicle longitudinal speed V_x (b) Brake Pressure for all wheels and (c) 6-input estimation results ($V_0 dV_x \bar{\sigma}_i \bar{m}_v P_i dP_i$).

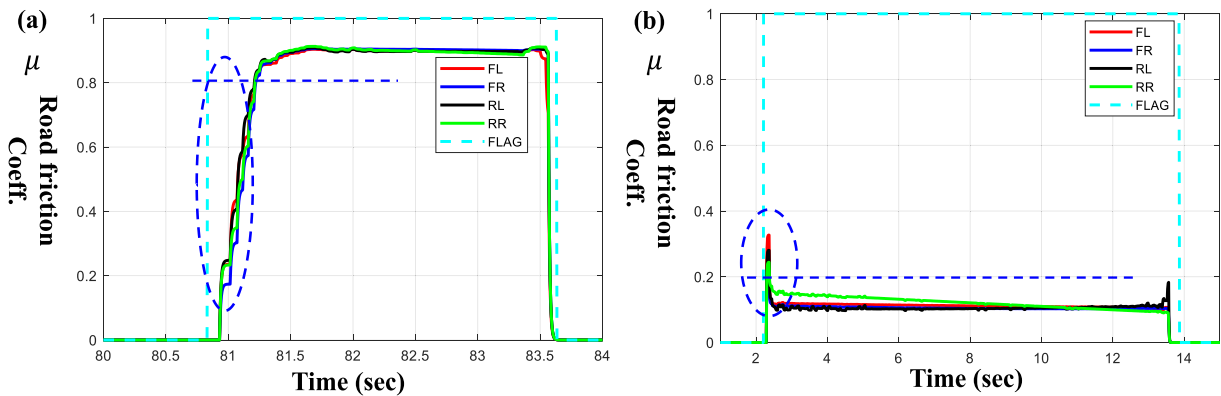


FIGURE 15. Example of Estimation result showing the limitation of proposed estimation scheme (a) Estimation results of asphalt road ($\mu > 0.8$) and (b) Estimation results of icy road ($\mu < 0.2$).

Specifically, Fig.7(a) and (b) indicate the longitudinal velocity of vehicle and brake line pressure for every wheel and, Fig.7(c) through (e) represent the estimation results of road friction coefficient for 4-input ANN classifier, 5-input ANN classifier, and 6-input ANN classifier, respectively.

The estimation result of 4-input ANN classifier is not accurate until the braking pressure of the wheel reaches 42 MPa, and the estimation becomes precise after the brake pressure becomes high enough to induce a condition in which the vehicle decelerates rapidly and the wheels enter into the regime that the maximum static road friction can be evident

(i.e., corresponding to the moment the vehicle slows down to a speed equal to 82% of the speed, 50 km/h, at which braking was initiated). However, the other ANN classifiers produce the quick and accurate estimates before the brake pressures of wheels reach up to 42 MPa (via 4-input classifier), which are 33 MPa (at 90% of 50km/h) and 30 MPa (93% of 50km/h), respectively. According to the results, we can see that the 6-input ANN classifier achieves more desirable estimate compared to the 5-input ANN classifier. This means that the 6-input of the ANN classifier including dP_i is more beneficial since it contains not only the magnitude of brake

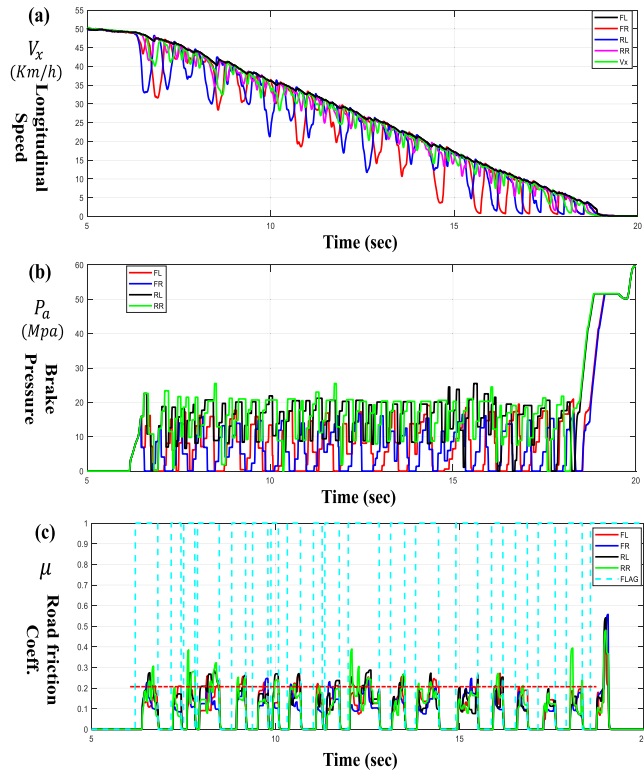


FIGURE 16. Estimation results of icy road($\mu < 0.2$) for braking at $V_0 = 50\text{km/h}$ under ABS operation (a) Vehicle longitudinal speed V_x (b) Brake Pressure for all wheels, and (c) 6-input estimation results ($V_0 dV_x \bar{\sigma}_i \bar{m}_v P_i dP_i$).

pressure, but also the gradient of the brake pressure, i.e. how quickly the pressure changes. Moreover, we can observe that the estimation results of 5- and 6-input classifiers are smoother than 4-input ANN classifier's since they include the direct braking scenario in estimation process (i.e. the evolution of estimates over a time shown in Fig.7(d) and (e) are quite similar to the brake pressure's displayed in Fig.7(b)).

Fig.8 describes the estimation results of asphalt road ($\mu > 0.8$) for braking at $V_0 = 80\text{km/h}$. Similar to the results of Fig.6, the 5- and 6-input ANN classifiers generate the accurate estimation results at low brake pressure below 30MPa, and the 6-input ANN classifier shows better responses than any other ANN classifiers. Specifically, the 4-input ANN classifier shows an estimate above 0.8 at a braking pressure above 42Mpa, and the other two classifiers perform the same task at 25Mpa and 28Mpa, respectively. This tendency is exactly synchronous with the results in Fig.3 and Fig.7. Fig.9 and Fig.10 include the estimation results of snowy road (ranging $0.2 < \mu < 0.5$) for braking at $V_0 = 45\text{km/h}$ and $V_0 = 80\text{km/h}$, respectively. According to the results of Fig.9 (c), we can observe that the estimate via 4-input ANN classifier quickly converged to the values ranging from 0.2 and 0.5, but is more irregular and fluctuating than other estimates' shown in Fig.9(d) and (e). In other words, other ANN classifiers (5- and 6-input) show smoother estimation responses as seen from Fig.9(d) and (e). Furthermore, this

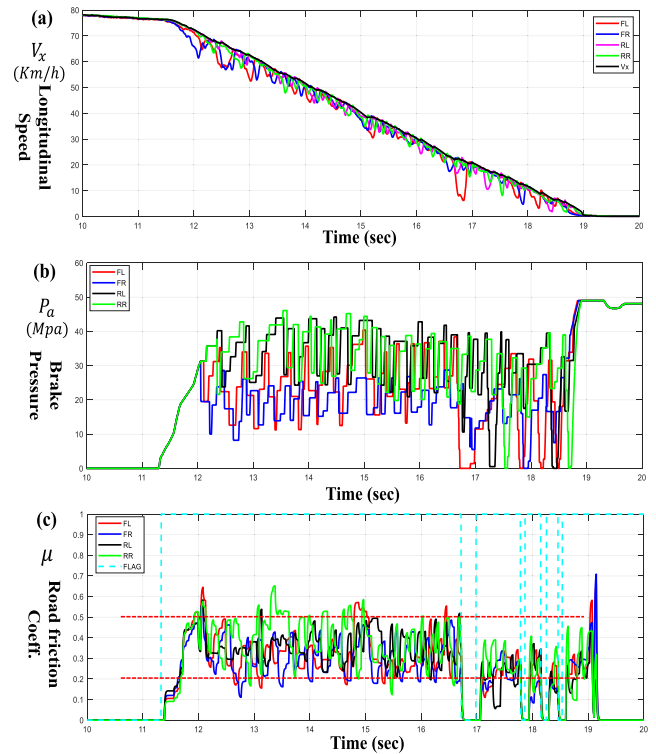


FIGURE 17. Estimation results of snowy road($0.2 < \mu < 0.5$) for braking at $V_0 = 80\text{km/h}$ under ABS operation (a) Vehicle longitudinal speed V_x (b) Brake Pressure for all wheels, and (c) Estimation results of 6-input ANN classifier ($V_0 dV_x \bar{\sigma}_i \bar{m}_v P_i dP_i$).

point of view can be shown more clearly from the results in Fig.10. All results of Fig.10 are smoothly and quickly fallen into the ranges from 0.2 to 0.5. It is obvious that both 5- and 6-input classifiers accomplish smoother results than ones via the 4-input classifier as seen from Fig.10 (c) through (e). If the estimates have to collaborate with any other advanced braking control system requiring the road/tire surface friction, the smooth results will be more desirable to achieve the unperturbed control. In this sense, it can be said that the 5- and 6-input cases become more beneficial than the 4-input case.

Fig.11 displays the estimation results of icy road ($\mu < 0.2$) for braking at $V_0 = 30\text{ km/h}$. According to Fig.11(c) through (e), it is found that the estimates reach the value 0.1, defined as the lowest μ in this study. However, the estimate of 4-input classifier contains fluctuations in itself compared to other results shown in Fig.11(d) and (e). This tendency was exactly matched with the results from Fig.7 through Fig.10. Also, the summary of outlier percentage for the results of Fig.7 through Fig.11 is presented in Table.3. According to the results of Fig.7 to Fig.11, it can be summarized that the original 4-input classifier guarantees a certain estimation performance, but adding the brake pressure and the corresponding gradient as the inputs to the classifier enables us to achieve more desirable level of estimation. In other words, first, both accurate and fast estimation can be made even under relatively lower

TABLE 3. Summary of outlier percentage for the results of Fig.6 through Fig.10.

| Case | Fig.7 ($\mu > 0.8$) | Fig.8 ($\mu > 0.8$) | Fig.9 ($0.2 < \mu < 0.5$) | Fig.10 ($0.2 < \mu < 0.5$) | Fig.11 ($\mu < 0.2$) |
|--------------------|--------------------------|--------------------------|--------------------------------|---------------------------------|---------------------------|
| Outlier percentage | 38% (4-input) | 29% (4-input) | 19% (4-input) | 17% (4-input) | 8% (4-input) |
| | 25% (5-input) | 20% (5-input) | 21% (5-input) | 0% (5-input) | 0% (5-input) |
| | 23%(6-input) | 19%(6-input) | 20%(6-input) | 5%(6-input) | 0%(6-input) |

TABLE 4. Summary of outlier percentage for the results of Fig.12 through Fig.14.

| Case | Fig.12 ($\mu > 0.8$) | Fig.13 ($0.2 < \mu < 0.5$) | Fig.14 ($\mu < 0.2$) |
|--------------------|---------------------------|---------------------------------|---------------------------|
| Outlier percentage | 12% | 8% | 10% |

TABLE 5. Summary of outlier percentage for the results of Fig.16 through Fig.19 (ABS on).

| Case | Fig.16 ($\mu < 0.2$) | Fig.17 ($0.2 < \mu < 0.5$) | Fig.18 (jump friction road) | Fig.19 (split friction road) |
|--------------------|---------------------------|---------------------------------|--------------------------------|---------------------------------|
| Outlier percentage | 17% | 18% | 31%(High) 22%(Low) | 32% (left) 25% (right) |

braking pressure conditions. Second, the results obtained by 5- and 6-input classifiers will be more useful for the collaboration with other control systems since it can ensure smoother estimation results. In this study, the validity of the 6-input ANN classifier was additionally investigated. Fig. 12, 13, and 14 show the estimated results for asphalt, snow, and icy roads, respectively, in the scenarios where the test vehicle is continuously (accelerated and) decelerated via braking. Estimates for each road reached to own true references within 0.25~0.36 seconds, although some outliers exist in early stage of braking (see Table.4 for more details). These results clearly demonstrate that the proposed 6-input ANN classifier produces robust and constant performance. However, even though 6-input ANN classifier shows an excellent performance, there still exist the limitations of the proposed method exhibiting an inaccurate result at the initial stage of braking (see the dotted-circle area as shown in Fig.15). Nevertheless, the proposed 6-input ANN classifier definitively guarantees the persistent estimation performance for the reference at the region right after the early stage of braking (earlier than the case with 4-input).

Furthermore, the effectiveness of proposed 6-input ANN classifier has been challenged by more extreme road conditions in which ABS should be activated most of the time during the braking process. Fig.16 presents the estimation results of icy road ($\mu < 0.2$) for braking at $V_0 = 50\text{km/h}$ under the ABS operation. Meanwhile, Fig.17 shows the estimation results of snowy road ($0.2 < \mu < 0.5$) for braking at $V_0 = 80\text{km/h}$ under ABS operation. As shown in Fig.16(b) and Fig.17(b), the brake pressure went on and off continuously until the vehicle is completely stopped. Consequently, the speeds of wheels go up and down due to the braking action as shown in Fig.16(a) and Fig.17(a). It can be seen from the results of Fig. 16(c) and Fig.17(c) that most of the estimates

belong to the desirable ranges of friction coefficients for icy roads and snowy roads, respectively. Fig.18 indicates the estimation results of the 6-input ANN classifier for the road suddenly changing from high to low friction conditions (i.e, jump from high to low, $\mu > 0.8$ to $\mu < 0.2$). According to the Fig.18(c), we can see that the estimates reach up to 0.8 around from 11.5 secs to 12.5 secs ($\mu > 0.8$ region) and go down below 0.2 from 14 secs to 21 secs ($\mu < 0.2$). Here, it should be mentioned that the estimate between 11.5 s and 12.5 s for the road $\mu > 0.8$ momentarily drops to the values 0.2~0.3 due to the low braking pressure below 6 Mpa, which falls in the unsuitable estimation region (i.e, the maximum friction coefficient hardly captures).

In Fig. 19, the estimation results for the split μ -road owning two different frictions in the left and right sides are presented (specifically, right: icy road ($\mu < 0.2$) and left: asphalt road ($\mu > 0.8$)). The vehicle is forced to be braking at $V_0 = 25\text{km/h}$ and ABS was consequently operated due to the road condition. It is found from Fig.19(c) that the estimates of left side wheels (i.e, FL and RL) are higher than the estimates of right wheels (i.e, FR and RR).

The estimate on the left side is approximately higher than 0.6 (approximately ranging from the values between 0.6 and 0.8) while the estimate on the right side is mostly lower than 0.3.

For even the extreme road surface condition like the split- μ road, the proposed ANN classifier still can distinguish one from another. However, the accuracy of the estimation is slightly unsatisfied (although this case will also be improved in the next study). Moreover, the summary of outlier percentage for the results of Fig.16 through Fig.19 is presented in Table.5. Furthermore, using the correlation coefficient below, the correlation of 6-input ANN classifier between estimate and true reference of each road for the results of Fig.7 through

TABLE 6. Correlation coefficient for the results of Fig.7 through Fig.14 (6-input classifier).

| | C.C for Fig.7 | C.C for Fig.8 | C.C for Fig.9 | C.C for Fig.10 | C.C for Fig.11 | C.C for Fig.12 | C.C for Fig.13 | C.C for Fig.14 |
|-------------|---------------|---------------|---------------|----------------|----------------|----------------|----------------|----------------|
| Front Left | 87% | 91% | 86% | 93% | 88% | 91% | 93% | 95% |
| Front Right | 88% | 92% | 88% | 93% | 87% | 92% | 89% | 93% |
| Rear Left | 87% | 91% | 87% | 92% | 88% | 90% | 92% | 92% |
| Rear Right | 89% | 91% | 86% | 92% | 88% | 87% | 90% | 93% |

TABLE 7. Correlation coefficient for the results of Fig.16 through Fig.19 (6-input classifier).

| | C.C for Fig.16 | C.C for Fig.17 | C.C for Fig.18 | C.C for Fig.19 |
|-------------|----------------|----------------|----------------|----------------|
| Front Left | 83% | 75% | 78% | 70% |
| Front Right | 82% | 76% | 80% | 72% |
| Rear Left | 83% | 75% | 79% | 78% |
| Rear Right | 84% | 75% | 79% | 75% |

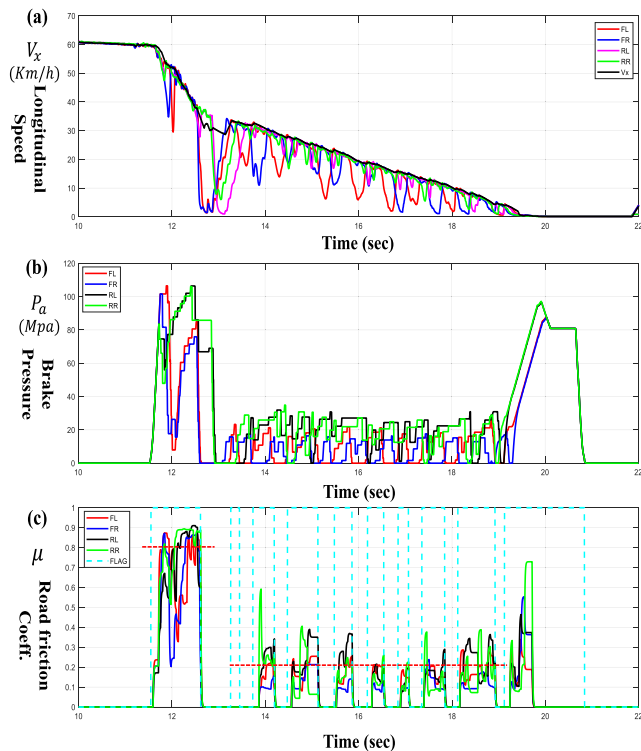


FIGURE 18. Estimation results of μ jump road (asphalt ($\mu > 0.8$) to icy ($\mu < 0.2$)) for braking at $V_0 = 60\text{km/h}$ under ABS operation (a) Vehicle longitudinal speed V_x (b) Brake Pressure for all wheels, and (c) Estimation results of 6-input ANN classifier ($V_0 d V_x \bar{\sigma}_i \hat{m}_v \hat{P}_i d \hat{P}_i$).

19 are summarized in Table.6 and Table.7.

$$C.C = \frac{n(\sum xy) - (\sum x)(\sum y)}{\sqrt{[n(\sum x^2) - (\sum x)^2][n(\sum y^2) - (\sum y)^2]}} \quad (6)$$

where n is the sample size, x is the true value of the concerned wheel, and y is the estimated value of the concerned wheel during brake. It can be seen from Table.6 and Table.7 that the estimation results capture 86~95% accuracy for

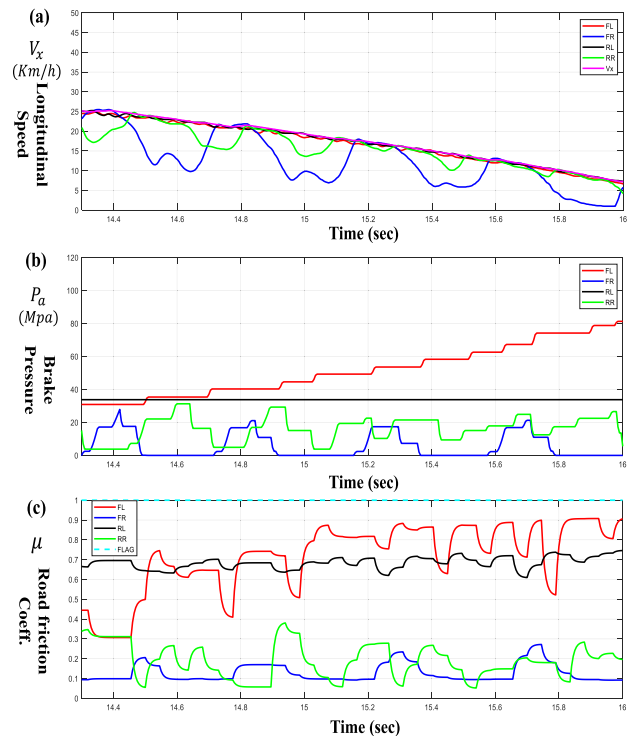


FIGURE 19. Estimation results of split μ road (Right: icy road ($\mu < 0.2$) and Left: asphalt road ($\mu > 0.8$)) for braking at $V_0 = 25\text{km/h}$ under ABS operation (a) Vehicle longitudinal speed V_x (b) Brake Pressure for all wheels, and (c) Estimation results of 6-input classifier ($V_0 d V_x \bar{\sigma}_i \hat{m}_v \hat{P}_i d \hat{P}_i$).

normal braking regardless of roads (Fig.7 through Fig.14) and 70~84 % accuracy for extreme road condition (Fig.16 through Fig.19), which should be further improved with more data in our next study.

IV. CONCLUSION

This paper validates the effectiveness of proposed ANN-based road friction classifier, which is our previous work [24], based on a field test data in SILS environment.

Additionally, the extension of input for the ANN classifier are discussed to obtain estimation results in better quality. The extended versions of classifiers include the braking pressure of each wheel (including the corresponding gradient), which is more intuitive and direct information of braking scenario than other inputs. Also, the braking pressure of each wheel is already available in current EUC due to the mandatory installation of ABS/ESP. Therefore, without any additional sensors, the modified ANN classifier can be implemented with slight change in classifier itself. Eventually, it is found that the proposed scheme was more suitable to obtain quicker and smoother estimation response compared to the previous approach (although the previous classifier can meet a certain level of estimation performance). In addition, including both brake pressure and the corresponding gradient into the input of ANN classifier can capture better and accurate estimation in even the condition that the applied brake pressure is relatively low. Even though the estimation performance during the normal braking is significantly improved by extending the input of the classifier, we must mention that there is still a room to supplement the estimation performance in early stage of normal braking, which will be explored in our next study.

In addition to the normal braking situation, we also investigated that, even extreme road conditions including split and jump friction roads under ABS operation, the proposed classifiers guarantee fairly accurate estimation performances, but should be further improved to achieve the better outcomes. Furthermore, our future studies should test and challenge the robustness of the proposed strategy for a wider variety of braking situations, and investigate its suitability with several advanced braking control systems demanding road friction coefficients (such as an AEB). Finally, we would like to say that, even in the trend that most road classifier heavily rely on deep learning techniques with an image processing, this work will inspire for ones who still wish to develop relatively-light, cost-effective, and simple-structured ANN classifier for road friction condition with data already available in most current automotive standards.

REFERENCES

- [1] F. Gustafsson, "Slip-based tire-road friction estimation," *Automatica*, vol. 33, no. 6, pp. 1087–1099, Jun. 1997.
- [2] S. Müller, M. Uchanski, and K. Hedrick, "Estimation of the maximum tire-road friction coefficient," *J. Dyn. Syst., Meas., Control*, vol. 125, no. 4, pp. 607–617, Dec. 2003.
- [3] K. Yi, K. Hedrick, and S.-C. Lee, "Estimation of tire-road friction using observer based identifiers," *Vehicle Syst. Dyn.*, vol. 31, no. 4, pp. 233–261, Apr. 1999.
- [4] K. Li, J. A. Misener, and K. Hedrick, "On-board road condition monitoring system using slip-based tire-road friction estimation and wheel speed signal analysis," in *Proc. ASME Int. Mech. Eng. Congr. Expo.*, Jan. 2006, pp. 267–276, doi: [10.1115/IMECE2006-14102](https://doi.org/10.1115/IMECE2006-14102).
- [5] J. Wang, L. Alexander, and R. Rajamani, "Friction estimation on highway vehicles using longitudinal measurements," *J. Dyn. Syst., Meas., Control*, vol. 126, no. 2, pp. 265–275, Jun. 2004.
- [6] D. Paul, E. Velenis, D. Cao, T. Dobo, and S. Hegarty, "Tyre-road friction μ -estimation based on braking force distribution," *Proc. Inst. Mech. Eng., D. J. Automobile Eng.*, vol. 233, no. 8, pp. 2030–2047, Jul. 2019.
- [7] C. Lee, K. Hedrick, and K. Yi, "Real-time slip-based estimation of maximum tire-road friction coefficient," *IEEE/ASME Trans. Mechatronics*, vol. 9, no. 2, pp. 454–458, Jun. 2004.
- [8] G. Cui, J. Dou, S. Li, X. Zhao, X. Lu, and Z. Yu, "Slip control of electric vehicle based on tire-road friction coefficient estimation," *Math. Problems Eng.*, vol. 2017, pp. 1–8, Nov. 2017.
- [9] M. Sharifzadeh, A. Senatore, A. Farnam, A. Akbari, and F. Timpone, "A real-time approach to robust identification of tyre-road friction characteristics on mixed- μ roads," *Vehicle Syst. Dyn.*, vol. 57, no. 9, pp. 1338–1362, Sep. 2019.
- [10] J. Hu, S. Rakheja, and Y. Zhang, "Real-time estimation of tire-road friction coefficient based on lateral vehicle dynamics," *Proc. Inst. Mech. Eng., D. J. Automobile Eng.*, vol. 234, nos. 10–11, pp. 2444–2457, Sep. 2020.
- [11] X. Ping, S. Cheng, W. Yue, Y. Du, X. Wang, and L. Li, "Adaptive estimations of tyre-road friction coefficient and body's sideslip angle based on strong tracking and interactive multiple model theories," *Proc. Inst. Mech. Eng., D. J. Automobile Eng.*, vol. 234, no. 14, pp. 3224–3238, Dec. 2020.
- [12] Y. Wang, J. Hu, F. Wang, H. Dong, Y. Yan, Y. Ren, C. Zhou, and G. Yin, "Tire road friction coefficient estimation: Review and research perspectives," *Chin. J. Mech. Eng.*, vol. 35, no. 1, pp. 1–11, Dec. 2022.
- [13] F. Holzmann, M. Bellino, R. Siegart, and H. Bubb, "Predictive estimation of the road-tire friction coefficient," in *Proc. IEEE Conf. Comput. Aided Control Syst. Design, IEEE Int. Conf. Control Appl., IEEE Int. Symp. Intell. Control*, Oct. 2006, pp. 885–890.
- [14] Y. Sato, D. Kobayashi, I. Kageyama, K. Watanabe, Y. Kuriyagawa, and Y. Kuriyagawa, "Study on recognition method for road friction condition," *JSAE Trans.*, vol. 38, no. 2, pp. 51–56, Jan. 2007.
- [15] M. Yamada, K. Ueda, I. Horiba, S. Tsugawa, and S. Yamamoto, "Road surface condition detection technique based on image taken by camera attached to vehicle rearview mirror," *Rev. Automot. Eng.*, vol. 26, no. 2, pp. 163–168, 2005.
- [16] W. R. Pasterkamp and H. B. Pacejka, "Optimal design of neural networks for estimation of tyre/road friction," *Vehicle Syst. Dyn.*, vol. 29, pp. 312–321, Jan. 1998.
- [17] T. Nakatsuji, I. Hayashi, A. Kawamura, and T. Shirakawa, "Inverse estimation of friction coefficients of winter road surfaces: New considerations of lateral movements and angular movements," *Transp. Res. Rec., J. Transp. Res. Board*, vol. 1911, no. 1, pp. 149–159, Jan. 2005.
- [18] X. Zhang and D. Göhlich, "A hierarchical estimator development for estimation of tire-road friction coefficient," *PLoS One*, vol. 12, no. 2, Feb. 2017, Art. no. e0171085.
- [19] A. M. Ribeiro, A. Moutinho, A. R. Fioravanti, and E. C. de Paiva, "Estimation of tire-road friction for road vehicles: A time delay neural network approach," *J. Brazilian Soc. Mech. Sci. Eng.*, vol. 42, no. 1, p. 4, Jan. 2020.
- [20] Z. Pu, Z. Cui, S. Wang, Q. Li, and Y. Wang, "Time-aware gated recurrent unit networks for forecasting road surface friction using historical data with missing values," *IET Intell. Transp. Syst.*, vol. 14, no. 4, pp. 213–219, Apr. 2020.
- [21] E. Šabanovič, V. Žuraulis, O. Prentkovskis, and V. Skrickij, "Identification of road-surface type using deep neural networks for friction coefficient estimation," *Sensors*, vol. 20, no. 3, p. 612, Jan. 2020.
- [22] P. Scott and J. Wang, "Machine-learning based tire-road friction prediction for ground vehicles," *IFAC-PapersOnLine*, vol. 55, no. 37, pp. 217–222, 2022.
- [23] J. B. W. Midgley, J. Fleming, and M. Otoofi, "Model-free road friction estimation using machine learning," in *Proc. IEEE Int. Conf. Mechatronics (ICM)*, Mar. 2023, pp. 1–7.
- [24] N. N. Minh and D. Jung, "Integrated estimation strategy of brake force cooperated with artificial neural network based road condition classifier and vehicle mass identification using static suspension deflections," *Appl. Sci.*, vol. 12, no. 19, p. 9727, Sep. 2022.



DAEYI JUNG received the Ph.D. degree from the Department of Mechanical Engineering, University of Tennessee, Knoxville, USA, in 2012. He is currently an Associate Professor with the Department of Mechanical Engineering, Kunsan National University (KSNU), South Korea. He was a Senior Researcher with Samsung Electronics and Hyundai-Motors for several years and has been with Kunsan National University, since 2017. His research interest includes controls and analysis of nonlinear systems.

• • •